

The role of parietal beta-band activity in the resolution of visual crowding

Giuseppe Di Dona^{a,b,1,*}, Denisa Adina Zamfira^{a,b,1}, Martina Battista^{a,c}, Luca Battaglini^d, Daniela Perani^{a,b}, Luca Ronconi^{a,b,*}

^a Division of Neuroscience, IRCCS San Raffaele Scientific Institute, Via Olgettina 60, 20132 Milano MI, Italy

^b School of Psychology, Vita-Salute San Raffaele University, Via Olgettina 58, 20132 Milano MI, Italy

^c MoMiLab Research Unit, IMT School for Advanced Studies Lucca, Piazza S. Francesco 19, 55100 Lucca LU, Italy

^d Dipartimento di Psicologia Generale, University of Padova, Via Venezia 8, 35131 Padova PD, Italy

ARTICLE INFO

Keywords:

Vision
Attention
EEG
tACS
Neural oscillations
Parietal cortex

ABSTRACT

Visual crowding is the difficulty in identifying an object when surrounded by neighbouring flankers, representing a bottleneck for object perception. Crowding arises not only from the activity of visual areas but also from parietal areas and fronto-parietal network activity. Parietal areas would provide the dorsal-to-ventral guidance for object identification and the fronto-parietal network would modulate the attentional resolution. Several studies highlighted the relevance of beta oscillations (15–25 Hz) in these areas for visual crowding and other conatural visual phenomena. In the present study, we investigated the differential contribution of beta oscillations in the parietal cortex and fronto-parietal network in the resolution of visual crowding. During a crowding task with letter stimuli, high-definition transcranial Alternating Current Stimulation (tACS) in the beta band (18 Hz) was delivered bilaterally on parietal sites, on the right fronto-parietal network, and in a sham regime. Resting-state EEG was recorded before and after stimulation to measure tACS-induced aftereffects. The influence of crowding was reduced only when tACS was delivered bilaterally on parietal sites. In this condition, beta power was reduced after the stimulation. Furthermore, the magnitude of tACS-induced aftereffects varied as a function of individual differences in beta oscillations. Results corroborate the link between parietal beta oscillations and visual crowding, providing fundamental insights on brain rhythms underlying the dorsal-to-ventral guidance in visual perception and suggesting that beta tACS can induce plastic changes in these areas. Remarkably, these findings open new possibilities for neuromodulatory interventions for disorders characterised by abnormal crowding, such as dyslexia.

1. Introduction

Visual crowding is the primary bottleneck for visual object perception (Levi, 2008; Pelli, 2008). It refers to the difficulty in discriminating objects in the presence of neighbouring flankers. Crowding is clearly observable in peripheral vision and occurs both with simple objects such as gabor patches (Levi et al., 2002) and more complex configurations, such as faces (Sun and Balas, 2015), letters (Whitney and Levi, 2011), and natural scenes (Ringer et al., 2021).

Two classic accounts have tried to explain crowding (Chakravarthi and Cavanagh, 2009). The bottom-up accounts posit that crowding stems from an incorrect integration of visual features following their detection (Parkes et al., 2001; Pelli et al., 2004). The top-down account, instead, explains crowding as a result of the limits of the attentional

capacity at given locations (He et al., 1996; Intriligator and Cavanagh, 2001). Accordingly, visual crowding involves both low and high associative visual areas depending on object complexity (Freeman and Simoncelli, 2011; Pelli, 2008).

Importantly, crowding does not seem to arise solely from the activity of visual areas. In particular, the magnocellular-dorsal (M-D) stream which connects the retina to occipital and parietal cortices (Maunsell and Newsome, 1987), traditionally involved in visual motion perception (Battelli et al., 2007; Braddick et al., 2003; Donner et al., 2007; Morrone et al., 2000), is also involved in visual crowding (Atilgan et al., 2020). The M-D stream has a central role for contour integration and segregation of visual stimuli in normal vision (Chakravarthi and Pelli, 2011), and consequently for complex visual tasks such as reading (Bertoni et al., 2019; Zorzi et al., 2012). Specifically, fast bottom-up projections to the

* Corresponding author at: Division of Neuroscience, I.R.C.C.S San Raffaele Hospital, Via Olgettina 60, 20132 Milano MI, Italy.

E-mail addresses: giuseppe.didona@gmail.com, didona.giuseppe@hsr.it (G. Di Dona), ronconi.luca@univr.it (L. Ronconi).

¹ These authors contributed equally to this work

M-D stream would provide low-frequency spatial representations facilitating attention-demanding slow identification in the ventral stream via recursive feedback from the parietal cortex (Levy et al., 2010; Vidya-sagar and Pammer, 2010). This dorsal-to-ventral communication would promote the activation of receptive fields of appropriate size, resulting in an effective segregation of target and flanker objects (Lamme and Roelfsema, 2000). However, given the poor resolution of coarse representations conveyed by the dorsal stream, the information coming from the parietal cortex may erroneously promote binding between target and flankers' features (Chakravarthi and Pelli, 2011).

The M-D stream also projects from early visual cortices to prefrontal cortices in primates (Goldman-Rakic and Porrino, 1985; Rempel-Clower and Barbas, 2000) and specifically to the inferior frontal gyrus in humans (Miller and Cohen, 2001). Low-level coarse visual representations are rapidly projected from early visual areas to the prefrontal cortex, which then conveys an initial guess of the image back to the ventral stream regions including the temporal cortex (Bar et al., 2001, 2006). In addition, different studies provided evidence for the involvement of the fronto-parietal network in visual attention (Boshra and Kastner, 2022; Corbetta et al., 2008; Corbetta and Shulman, 2002; Giesbrecht et al., 2003; Szczepanski et al., 2010), which could modulate many visual phenomena, including crowding (Albonico et al., 2018; Bacigalupo and Luck, 2015; Chen et al., 2014, 2014; Fortenbaugh et al., 2015; Kewan-Khalayly et al., 2022).

In general, bottom-up and top-down accounts posit that crowding depends on different, interacting, neural networks. Within this debate, electroencephalography (EEG) provided converging evidence using Vernier stimuli (Chicherov et al., 2014), letters (Peng et al., 2018) or letters-like Gabor configurations (Ronconi et al., 2016) that crowding induces a suppression of the N1 component (200–250 ms post-stimulus) across parietal and/or occipital sensors, compatible with an influence on later visual processing stages. Other EEG evidence (Han and Luo, 2019) isolated target- and flanker-specific EEG activity in a visual crowding task via a temporal response function, reporting an early-starting occipital component and a later-occurring fronto-parietal one. Only the latter was correlated with the behavioural performance in the crowding task and exerted causal influence on the occipital component, as assessed via a directed connectivity analysis. These results suggest that the activation of the fronto-parietal network reflects a top-down modulation during visual crowding.

Other EEG studies focused on the analysis of the oscillatory activity, reported that crowding and other connatural visual phenomena show a relationship with beta-band activity (15–25 Hz) (Di Dona and Ronconi, 2023). Modulations of beta-band oscillations have been associated with perceptual reorganisation (Ehm et al., 2011; Kornmeier and Bach, 2012; Okazaki et al., 2008), for example during perceptual switch between global and local motion perception (and vice-versa) (Romei et al., 2011; Zaretskaya and Bartels, 2015). Importantly, in a visual crowding task employing letter stimuli, larger post-stimulus beta power reduction was observed in a strong crowding with respect to a weak crowding condition (Ronconi et al., 2016). In addition, a correct response in the same task was linked to stronger pre-stimulus beta power (Ronconi and Bellacosa Marotti, 2017). The association of beta oscillations to visual crowding was further strengthened by Battaglini and colleagues (Battaglini et al. 2020a), who applied transcranial Alternating Current Stimulation (tACS) on the right parietal cortex at frequencies within the beta (18 Hz) and alpha (10 Hz) bands, or in a sham (placebo) regime. Only beta-band tACS ameliorated performance in a visual crowding task in the contralateral hemifield and, moreover, increased post-tACS beta-band power in resting-state EEG (RS-EEG). Together, these results provide robust evidence about the central role of right parietal beta oscillations in visual crowding. Despite classical models suggested that the right is more specialised than the left hemisphere in the control of visual attention (Corbetta and Shulman, 2011), however, whether visual crowding itself is specifically associated to the activity of the right parietal or of both parietal areas has never been tested.

At the same time, beta-band rhythmic communication within the right fronto-parietal network appears as having an evident role for visual perception and attention (Rogala et al., 2020; Yordanova et al., 2017), stimulating questions about its possible influence on visual crowding. For example, single-pulse TMS applied to frontal eye fields (FEF) triggers phase reset of beta oscillations at occipital sensors and modulates the accuracy of motion discrimination (Veniero et al., 2021). Consistently, rTMS at high beta frequency (30 Hz) applied to FEF resulted in higher inter-regional synchronisation in beta oscillations between FEF and bilateral parietal sensors and increased visual sensitivity in a visual detection task (Stengel et al., 2021). On the other hand, low beta rTMS (20 Hz) delivered to the right intraparietal sulcus or right FEF interfered with visual identification (Capotosto et al., 2009).

In our previous study (Battaglini et al. 2020a), we tested the effects of both alpha and beta tACS (as compared to sham tACS), but only beta tACS yielded behavioural modulation of visual crowding and changes in post-stimulation oscillatory activity. These results provided an important indication of frequency specificity. In the present study, we aimed at elucidating the different functional characterizations of beta oscillations in parietal cortices and in the right fronto-parietal network during visual crowding. Specifically, we investigated whether the improvements previously found by Battaglini and colleagues (Battaglini et al., 2020a) in reducing the impact of visual crowding with a right parietal stimulation, and limited to the contralateral visual hemifield, could be extended to both visual hemifields. First, given that the parietal lobe is a crucial hub of the dorsal attention network, we hypothesised that by extending the electrical stimulation to both parietal cortices, the beneficial effect on visual performance would be transferred to the entire visual field. However, given the well-established dominance of the right hemisphere for visuospatial attention (Heilman and Van Den Abell, 1980; Corbetta et al., 2000; Mengotti et al., 2020; Gallotto et al., 2022) and based on recent evidence showing the involvement of beta oscillations within the fronto-parietal network during several visual perception and attention tasks (Di Dona and Ronconi, 2023; Veniero et al., 2021; Yordanova et al., 2017), we investigated whether simultaneously stimulating the right parietal and frontal areas could similarly modulate visual crowding performance across the entire visual field.

2. Materials and methods

2.1. Participants

Twenty-five healthy adults (14 F, Mean Age = 20.3, Age Range = 18–26) with normal or corrected to normal vision and normal hearing were recruited. All participants met the criteria for the application of transcranial Alternating Current Stimulation (tACS) (Antal et al., 2017). The study protocol was approved by the Ethical Committee of San Raffaele Hospital and performed in accordance with the Helsinki Declaration of Human Studies and all participants signed the informed consent prior to participating in the study. A power analysis was performed in GPower (Erdfelder et al., 1996) software to estimate the minimum sample size to reach 0.80 power for a two-tailed paired sample *t*-test with an effect size of $d = 0.6$ drawn from a previous similar study (Battaglini et al., 2020a). Such analysis showed that 24 participants were needed. After excluding 3 participants (*see section Behavioural data preprocessing and model fitting*), a power of ~ 0.775 was estimated for 22 participants.

2.2. Stimuli and procedure

Stimuli for the crowding task consisted of letter-like configurations (H for flankers and T for the target) composed by Gabor patches and covering an area of 1.5×1.5 deg each. They were created using Psychtoolbox in MATLAB (Brainard, 1997) and presented on a 20" LCD Dell monitor (1600 \times 900 pixels; 60 Hz refresh rate) with a grey background (40 cd/m²). For details about the stimuli composition see the

Supplementary Materials.

The entire experimental procedure (task, EEG and tACS) was done in a dimly lit room. In each trial, a fixation point (2 s) anticipated the target letter T (50 ms), which appeared at 11 deg of eccentricity in the right or left visual hemifield with 4 equiprobable orientations (0°, 90°, 180°, 270°). Target duration prevented saccades towards the target. Two flanker letters H were positioned above and under the target letter T and at 7 equiprobable distances (1.90, 2.27, 2.65, 3.02, 3.40, 3.78, or 4.15 deg). A blank screen (2 s) followed the presentation of the letters' array and anticipated the response display, in which participants were asked to report the letter T orientation using the keyboard. 1 s after the response was given, a subsequent trial started.

Each participant repeated the task in three different non-consecutive days under three stimulation conditions, randomised across participants: 18 Hz stimulation with a Bilateral Parietal montage (BP-tACS), 18 Hz stimulation with a Fronto-Parietal right montage (FP-tACS), and Sham. The precise stimulation frequency (18 Hz) was chosen based on our previous studies because it exhibited the maximum crowding-induced modulation (Battaglini et al., 2020a; Ronconi et al., 2016; Ronconi and Bellacosa Marotti, 2017). In each session, eyes-closed RS-EEG was acquired for 4 min before and after performing the task.

Each session lasted 40 min. Participants were not aware of the specific stimulation protocol of each session (single blind); they completed on average 479 ± 35 trials per session (1st session: Mean = 464, SD = 32; 2nd session: Mean = 478, SD = 38; 3rd session: Mean = 494, SD = 28). After each session, participants filled a questionnaire to evaluate their sensations during the stimulation (Fertonani et al., 2015) (see Supplementary Materials).

2.3. Behavioural data preprocessing and model fitting

Correct responses were calculated separately for each participant and experimental conditions (i.e. left/right hemifield; Sham/BP-tACS/FP-tACS stimulation) and modelled with a logistic function using the R package quickpsy (Linares and López i Moliner, 2016) to extract slope and threshold values (see Supplementary Materials). Three participants were excluded from behavioural data analyses as their fitted functions showed unexpected inverse patterns predicting higher accuracy for higher levels of visual crowding. Therefore, statistical analyses were performed on 22 participants.

2.4. EEG recording, tACS stimulation and preprocessing

We recorded RS-EEG with a StarStim system (Neuroelectronics, Inc.) using a neoprene cap to place the following 32 electrodes: Fp1, Fp2, F7, F3, Fz, F4, F8, FC5, Fc1, FC2, FC6, T7, C3, Cz, C4, T8, CP5, CP1, CP2, CP6, P7, P3, Pz, P4, P8, PO7, PO3, PO4, PO8, O1, Oz, O2. We used 23 Ag/AgCl EEG-only electrodes and 9 Ag/AgCl hybrid tACS/EEG electrodes (1 cm radius). In the BP-tACS condition, stimulation electrodes were placed in P4 and P3, while return electrodes were placed in C4, P8, O2, Pz, C3, P7, O1. All the remaining electrodes were used only for EEG recording. This bi-focal high-definition montage optimally stimulated both the right and the left parietal cortices (Fig. 1). In the FP-tACS condition, stimulation electrodes were F4 and P4, while return electrodes were Fp2, Fz, F8, C4, P8, O2, and Pz. All the remaining electrodes were used only for EEG. This bi-focal high-definition montage stimulated the right fronto-parietal network (Fig. 1). In both stimulation conditions, the peak-to-baseline intensity of the stimulating electrodes was set at 0.8 mA with 0° phase, while the intensity of return electrodes was put to 0.228 mA with 180° phase. Stimulation intensity was chosen following the tACS safety guidelines (Antal et al., 2017). The total dosage of BP-tACS and FP-tACS protocols was 2749.2 mC (micro-Coulomb) for 40 min of stimulation. In the sham protocol, 18 Hz tACS stimulation was delivered only for 30 s at the beginning and at the end of the task with ramped-up/down intensity.

EEG signal was recorded at 500 Hz. Signal was referenced online to

the right earlobe. For stimulation electrodes impedance was <10 kΩ. For EEG electrodes, the Quality Index² computed by NIC2 software was kept between 0 and 0.5 (highest rank).

RS-EEG data were preprocessed using EEGLAB (Delorme and Makeig, 2004), applying bandpass filtering (0.05 - 80 Hz), average re-reference, downsampling (250 Hz), and a notch filter (50 Hz). Signal was then divided into 1 s epochs. Epochs exceeding ± 100 μ V amplitude in any of the channels were rejected. Noisy channels were interpolated. ICA was run on the signal using the Infomax algorithm (Bell and Sejnowski, 1995). Ocular artefacts were identified with ICLabel and removed (Pion-Tonachini et al., 2019). Epochs containing excessive noise were manually rejected. The FFT power spectrum between 1 and 40 Hz was computed using a Hanning taper zero-padded to a length of 4 s via FieldTrip toolbox (Oostenveld et al., 2011). The "Fitting Oscillations and One-Over-F" (FOOOF) (Donoghue et al., 2020) toolbox was used to distinguish between the "full" and the "periodic" (oscillatory) or "aperiodic" (1/f) power spectra. Next, power values in the alpha (8–12 Hz) and beta (15–25 Hz) bands were extracted from the full and the periodic power spectra. Power values between 1 and 40 Hz were extracted from aperiodic power spectrum. One participant was excluded from EEG analyses as his/her data were corrupted; thus, statistical analyses were performed on 24 participants.

2.5. Statistical analysis

2.5.1. Behavioural data analysis

To evaluate the effect of tACS on visual crowding, thresholds and slope values were analysed via repeated-measures ANOVA with two within-subjects factors: Condition (Sham, BP-tACS, FP-tACS) and Hemifield (left, right). Post-hoc *t*-tests were performed to explore main effects or interactions and all *p*-values were then FDR corrected.

2.5.2. EEG changes induced by tACS

Power values extracted from the full and the periodic power spectra of the pre-stimulation RS-EEG were compared with the power values of the post-stimulation RS-EEG within each band (alpha, beta) across the whole scalp using non-parametric permutation tests with cluster-based correction for multiple comparisons (Maris and Oostenveld, 2007). Aperiodic power was analysed in the same way between 1 and 40 Hz. *P*-values were further FDR-corrected for each analysis.

2.5.3. Exploring the nature of tACS-induced EEG aftereffects

To understand whether tACS-induced EEG aftereffects could be attributable either to carry-over phenomena echoing online tACS effects (Helfrich et al., 2014b; Laczó et al., 2012; Strüber et al., 2014) or to tACS-induced synaptic plasticity emerging mostly offline (Veniero et al., 2015; Vossen et al., 2015; Wischniewski and Schutter, 2017; Zaehle et al., 2010), a follow-up analysis was performed. Specifically, we investigated whether the strength of beta-band activity modulations in RS-EEG (before vs. after tACS stimulation), hereafter referred to as tACS-induced aftereffects, depends on: i) "individual beta frequency" (IBF), ii) stimulation frequency (SF) and iii) the difference between IBF and SF for the tACS conditions in which aftereffects emerged.

Two separate linear models were implemented. For the first model, IBF was computed in each individual participant as the frequency with higher beta power from the power spectrum (FOOOF-corrected) of RS-EEG acquired before each tACS session (separately for each channel and condition, only considering channels in which an aftereffect was recorded). Then, power values of the difference between RS-EEG acquired before and after each tACS session were extracted at ± 2 , ± 1.5 , ± 1 , ± 0.5 and 0 Hz distance from IBF and also from SF in each individual participant. For the second model power values were extracted only at

² This index depends on line noise power at 50 Hz (μ V²), main noise power of the standard EEG 1-40 Hz band (μ V²), offset (mean value of the waveform).

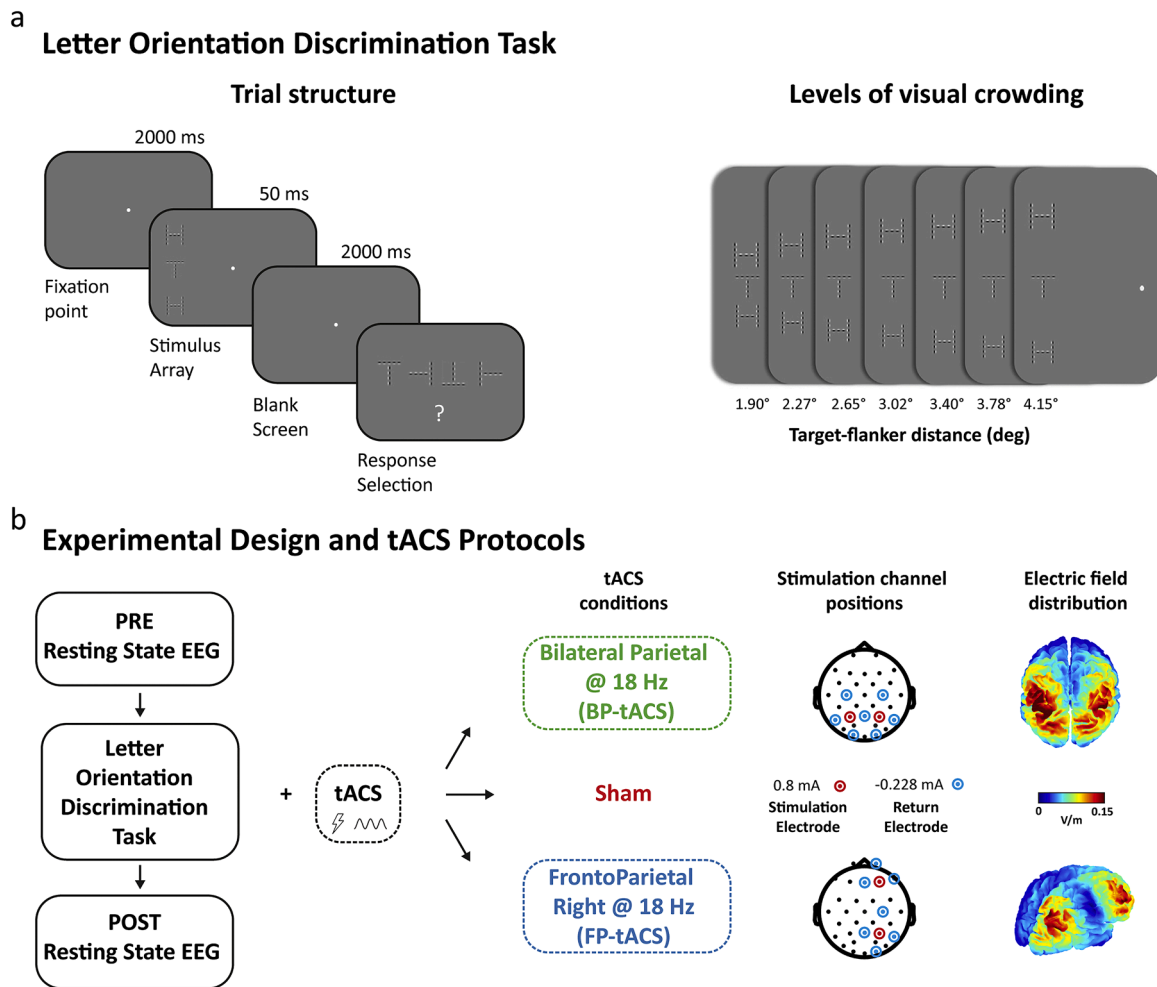


Fig. 1. a) Trial structure and levels of visual crowding of the Letter Orientation Discrimination Task. b) Experimental design and tACS protocols.

IBF and the difference between IBF and SF (18 Hz) was computed. ANOVAs were run on each model. Post-hoc tests were run to explore possible interaction effects via the 'emmeans' package (Lenth et al., 2018) and all p-values were then FDR corrected.

2.5.4. Exploring the link between tACS-induced behavioural and neurophysiological effects

To understand possible links between tACS-induced behavioural and neurophysiological modifications, several correlations were computed. In particular, Pearson's ρ was computed within each condition between the behavioural threshold and alpha power, beta power, aperiodic exponent and offset recorded before and after the stimulation as well as their differential (i.e., post-pre). Alpha & beta power, as well as exponent and offset values were computed from bilateral parieto-occipital channels (P3, Pz, P4, P7, P8, PO3, PO4, PO7, PO8, O1, Oz, O2) in which the majority of physiological effects found in the present work emerged and then averaged across channels. Importantly, exponent and offset parameters were used instead of aperiodic power as this last metric was computed only to check for possible modulations of aperiodic activity but has no functional meaning per se. All p-values were then FDR corrected.

3. Results

3.1. Behavioural results

The RM-ANOVA on thresholds values showed a main effect of

Condition ($F_{2,42} = 4.33, p = .019, \eta^2 = 0.013$). Post-hoc *t*-tests (FDR-corrected) revealed a lower threshold in the BP-tACS condition with respect to Sham ($t_{21} = -2.30, p_{FDR} = 0.046, d = 0.28$) and FP-tACS ($t_{21} = -2.67, p_{FDR} = 0.042, d = 0.26$). The main effect of Hemifield ($F_{1,21} = 0.15, p = .69$) and the interaction between Hemifield and Condition ($F_{2,42} = 0.46, p = .63$) did not yield significant results. The RM-ANOVA on slope values showed no significant effects. Behavioural results are depicted in Fig. 2.

3.2. EEG results

3.2.1. Selective tACS-induced modulations of beta-band activity in bilateral parietal areas

When analyzing the full power spectrum, permutation tests between power values recorded before and after the stimulation in the beta band (15–25 Hz) revealed the presence of a significant negative cluster topographically distributed on bilateral parietal sensors both in the sham ($p_{FDR} = 0.003, 15\text{--}19.75$ Hz) and in the BP-tACS condition ($p_{FDR} = 0.002, 15\text{--}25$ Hz). No significant clusters were found for the FP-tACS condition (all $ps_{FDR} > 0.06$). The same test operated on the periodic power spectrum (FOOOF-corrected) showed a significant negative cluster on bilateral parietal sensors ($p_{FDR} = 0.049, 15\text{--}17.5$ Hz) only in the BP-tACS condition (Fig. 3c& 3f). No significant clusters were found for the sham and the FP-tACS conditions (all $ps_{FDR} > 0.08$). This indicates that aperiodic-adjusted (1/*f*-free) beta-band power was reduced in bilateral parietal sensors only for the BP-tACS condition.

The results of the same analysis on alpha activity are available on

Behavioural Results - Letter Orientation Discrimination Task

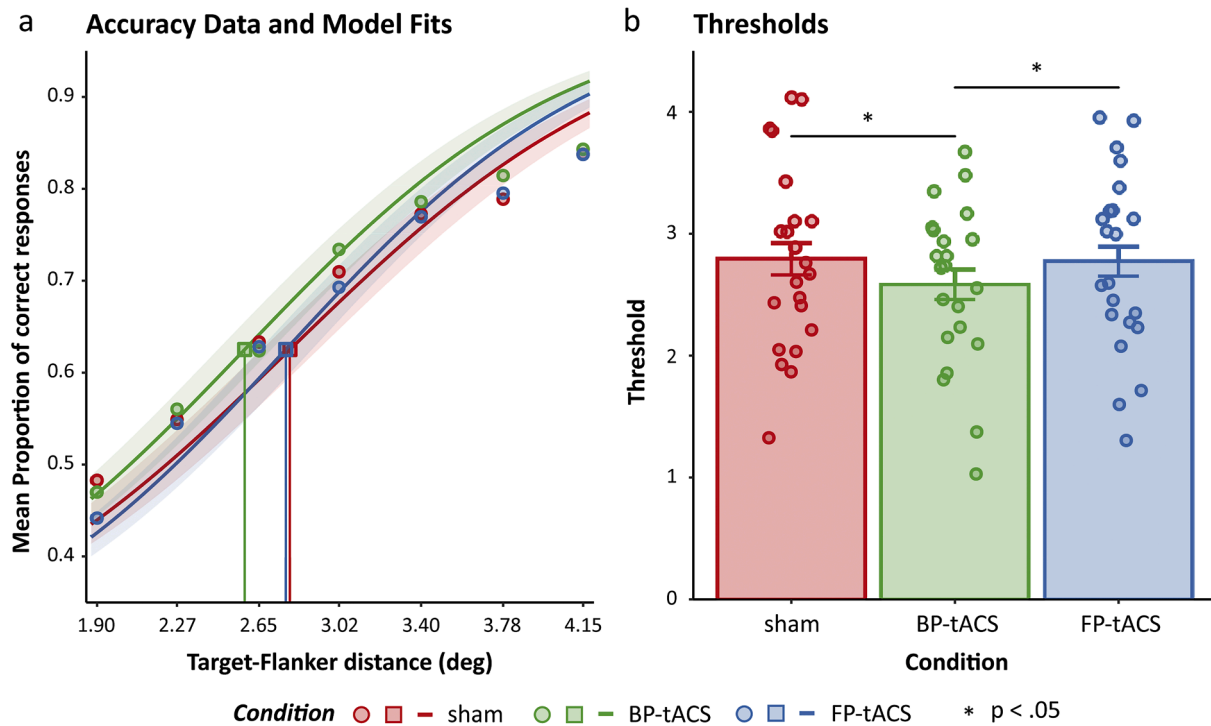


Fig. 2. Behavioural Results of the Letter Orientation Discrimination Task. a) Psychometric fits (curves) with SEM (shaded areas) obtained from the mean proportions of correct responses in the three conditions (red = sham, green = BP-tACS, blue = FP-tACS). Round dots represent the mean proportion of correct responses in function of target-flanker distance (x-axis) averaged across participants. Squared dots indicate behavioural thresholds (0.625 accuracy). Vertical lines indicate the projection of the threshold points onto the x-axis. b) Histograms represent threshold data averaged across participants with SEM bars and superimposed individual thresholds (round dots) for each condition (red = sham, green = BP-tACS, blue = FP-tACS). * indicates $p < .05$ (FDR corrected).

Supplementary Materials and depicted in Figs. 3.

3.2.2. Modulations of aperiodic activity is both task- and tACS- dependent

Permutation tests between power values recorded before and after the stimulation on the whole aperiodic spectrum (1–40 Hz) revealed the presence of a negative cluster in the sham ($pFDR = 0.010$, 1–15.75 Hz), in the BP-tACS ($pFDR = 0.009$, 2.75–40 Hz) and in the FP-tACS ($pFDR = 0.014$, 1.5–35.5 Hz) conditions (Fig. 3e). Thus, all conditions were characterised by a power reduction of aperiodic (1/f) activity but in a narrower band for the sham condition with respect to BP-tACS and FP-tACS conditions.

3.2.3. tACS-induced EEG aftereffects partially support spike timing dependent plasticity

The linear model $Power \sim Distance + Measure + Distance * Measure$ was fitted to RS-EEG data only in the BP-tACS condition, with Distance as continuous predictor (± 2 , ± 1.5 , ± 1 , ± 0.5 and 0 Hz from IBF or SF), and Measure as a categorical predictor (IBF, SF). Power was averaged across the channels of the significant cluster (PO4, O1, PO7, P3, P7) in BP-tACS condition. The model revealed an interaction effect between Distance and Measure ($F_{1,428} = 11.38$, $p < .001$). Post-hoc tests showed a significant difference in the slope of Distance between IBF and SF ($t_{428} = 3.37$, $p < .001$), revealing a significant positive slope for IBF ($t_{428} = 4.60$, $p < .001$) and a non-significant slope for SF ($p = .87$). These comparisons revealed that the aftereffects recorded in RS-EEG in the BP-tACS condition grew higher at frequencies lower than IBF (Fig. 4). A main effect of Distance ($F_{1,428} = 9.88$, $p = .001$) and a main effect of Measure ($F_{1,428} = 16.14$, $p < .001$) were found, but were not further analysed considering their involvement in the interaction explored above.

The linear model $Power \sim Difference(IBF-SF)$ was fitted to RS-EEG data only in the BP-tACS condition with $Difference(IBF-SF)$ as

continuous predictor expressing the difference between IBF and SF. The model did not show a significant effect of the difference between IBF and SF ($p = .54$).

3.3. Correlation analyses

The correlation analyses performed between behavioural performance and neurophysiological modulations did not yield any significant effect (all $ps > 0.07$). The complete table of the results is available in Supplementary Materials (Supplementary Table 5).

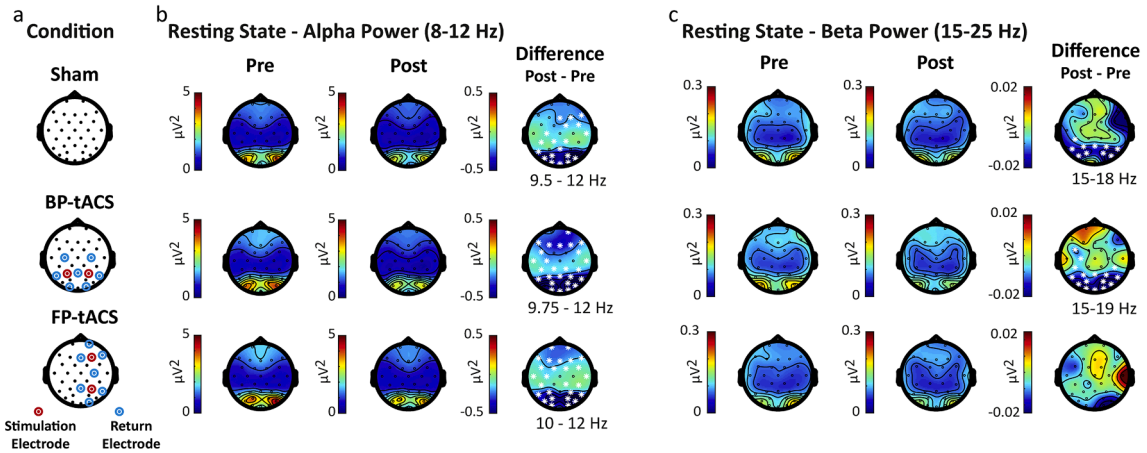
4. Discussion

4.1. Bilateral parietal beta tACS reduces the effects of visual crowding

The present study aimed at elucidating possible different functional characterisation of beta oscillations in parietal cortex and fronto-parietal networks via precise bifocal tACS.

The central behavioural finding of the present study is a lower threshold for letter orientation discrimination when 18 Hz tACS is applied to bilateral parietal cortices (BP-tACS condition) with respect to when the same stimulation is applied to the right fronto-parietal network (FP-tACS condition) and when no stimulation is applied (Figure 2). Given that we found a generalisation of the behavioural enhancement in the resolution of visual crowding to both visual hemifields only during the BP-tACS stimulation, it might be that the FP-tACS applied with 0 phase lag (in-phase) was not optimal to favour fronto-parietal communication, which may require an optimal amount of temporal delay. Based on previous evidence, one possibility is to investigate whether anti-phase stimulation (see Salamanca-Giron et al., 2021 & Yapple and Vakhrushev, 2018), or other optimal inter-stimulation

EEG Results - Resting State EEG



EEG Results - Resting State EEG decomposed in aperiodic and periodic activity

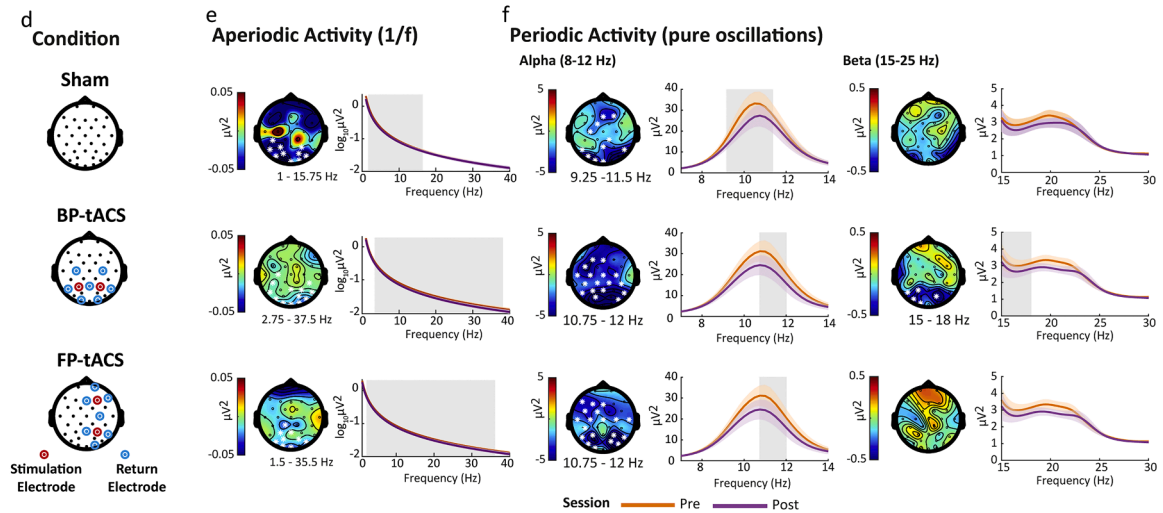


Fig. 3. EEG Results of the Resting State EEG (1st row). a) Stimulation layouts of the three conditions (sham, BP-tACS and FP-tACS). Stimulation electrodes are represented by red dots while return electrodes are represented by blue dots. Topographies represent power in the b) alpha band (8–12 Hz) and c) beta band (15–25 Hz) extracted from the FFT power spectrum recorded before (“Pre”, 1st column) and after the task (“Post”, 2nd column) as well as the difference (3rd column) between the two (calculated by subtracting power of the “Pre” session from the one recorded in the “Post” session). Channels that were included in the clusters are represented by white asterisk marks; the frequency bands in which significant clusters emerged are represented below the topographies. EEG Results of the Resting State EEG decomposed in aperiodic and periodic activity (2nd row). d) Stimulation layouts of the three conditions (sham, BP-tACS and FP-tACS). Stimulation electrodes are represented by red dots while return electrodes are represented by blue dots. e) Topographies (1st column) represent the power differences in the aperiodic activity of the RS-EEG recorded before and after the behavioural task in the frequency band in which significant clusters emerged (reported below each topography). Channels that were included in the clusters are represented by white asterisk marks. FFT power spectra (2nd column) of the aperiodic activity recorded before (“Pre”, orange line) and after (“Post”, violet line) the behavioural task averaged across P7, P3, Pz, P4, P8, PO7, PO3, PO4, PO8, O1, Oz, O2 channels expressed in $\log_{10}\mu\text{V}^2$ (for illustrative purposes). Shaded coloured areas represent SEM while shaded grey areas represent the frequency bands in which significant clusters emerged. f) Topographies represent the power differences in the periodic activity of the RS-EEG recorded before and after the behavioural task in the alpha (8–12 Hz, 1st column) and beta (15–25 Hz, 3rd column) bands. Channels that were included in the clusters are represented by white asterisk marks; the frequency bands in which significant clusters emerged are represented below the topographies. FFT power spectra of the periodic activity within alpha (2nd column) and beta (3rd column) bands recorded before (“Pre”, orange line) and after (“Post”, violet line) the behavioural task averaged across P7, P3, Pz, P4, P8, PO7, PO3, PO4, PO8, O1, Oz, O2 channels (for illustrative purposes). Shaded coloured areas represent SEM while shaded grey areas represent the frequency bands in which significant clusters emerged.

intervals, might promote efficient fronto-parietal communication inducing plastic changes in oscillatory activity and ameliorating performance in visual perception tasks. Moreover, frontal and parietal areas involved in visuo-spatial attention have been shown to be characterised by different natural frequencies within the beta band (Capilla et al., 2022; Di Dona and Ronconi, 2023). Therefore, it is possible that 18 hertz was a suboptimal frequency for targeting the frontal cortex and inducing significant neurophysiological and behavioural changes. However, since only correlational studies have been conducted, empirical studies are needed to better clarify these aspects from a causal perspective through

the use of neuromodulation.

Interestingly, this behavioural result was accompanied by a reduction of FOOOF-corrected beta power after BP-tACS stimulation, but not after sham or FP-tACS stimulation, as revealed by the analysis of “pure” oscillatory activity (Fig. 3f). These results argue for a functional predominance of beta oscillations over parietal cortices, in line with previous studies framing beta as the “natural” rhythm of parietal areas (Cabral-Calderin and Wilke, 2020; Capilla et al., 2022; Samaha et al., 2017). Moreover, they corroborate previous findings about the fundamental role of parietal beta oscillations for visual crowding (Battaglini

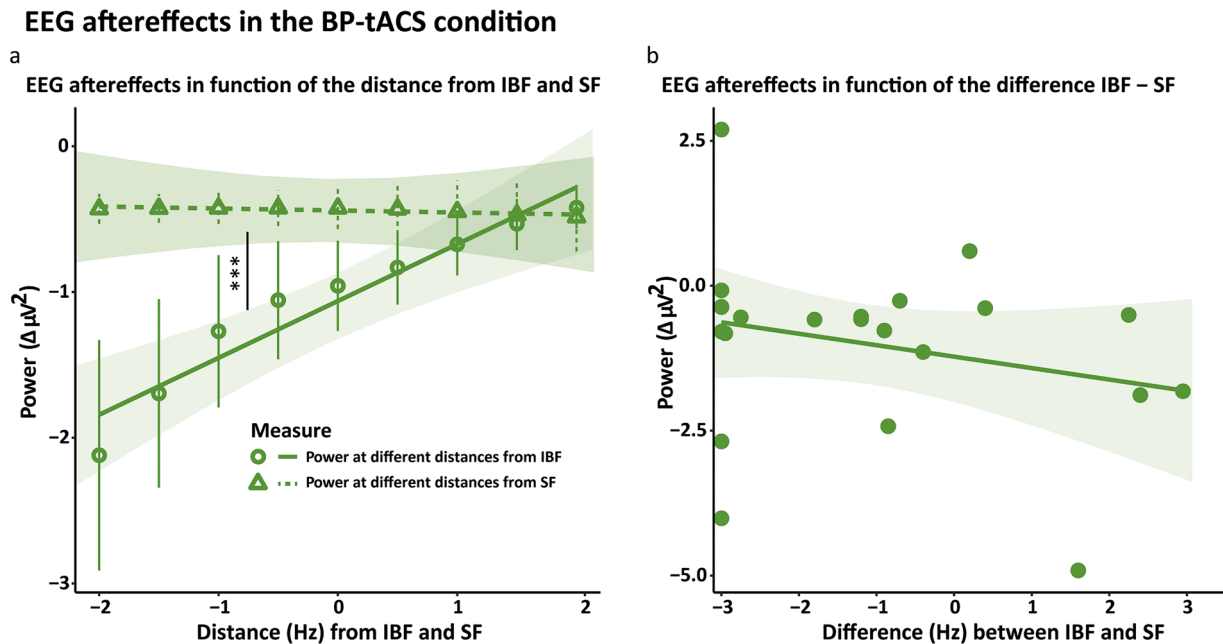


Fig. 4. EEG aftereffects calculated as the difference in beta power between RS-EEG recorded before and after 18 Hz bilateral parietal tACS over PO4, O1, PO7, P3, P7 electrodes. a) Hollow circles represent beta power calculated at ± 2 , ± 1.5 , ± 1 , ± 0.5 and 0 Hz distance from individual beta frequency (IBF) averaged across participants and electrodes, calculated as the frequency with higher beta power in each individual subject at each electrode. The solid line and the shaded area represent the prediction and confidence intervals of the associated linear model. Hollow triangles represent beta power calculated at ± 2 , ± 1.5 , ± 1 , ± 0.5 and 0 Hz distance from stimulation frequency (SF, 18 Hz) averaged across participants and electrodes. The dashed line and the shaded area represent the prediction and confidence intervals of the associated linear model. The asterisks indicate the level of significance $p < .001$ for the comparison between the slopes of the linear model. b) Full circles represent EEG aftereffects of individual participants calculated at individual beta frequency (IBF) and plotted in function of the difference between individual beta frequency and stimulation frequency (SF, 18 Hz). The solid line and the shaded area represents the prediction and confidence intervals of the associated linear model.

et al., 2020a; Ronconi et al., 2016; Ronconi and Bellacosa Marotti, 2017), and visual perception more generally (Costa et al., 2017; Zaretskaya and Bartels, 2015). These results are also consistent with the notion that crowding depends on an incorrect integration of target and flanker features (Parkes et al., 2001; Pelli, 2008) supported by a dorsal-to-ventral projection originating in parietal areas.

4.2. RS-EEG aftereffects of bilateral parietal 18 Hz tACS

Previous studies employing RS-EEG before and after behavioural tasks coupled with tACS showed contrastive results for power modulations within theta (Kleinert et al., 2017; Pahor and Jaušovec, 2018), alpha (Aktürk et al., 2022; Battaglini et al. 2020b; Wang et al., 2022) and beta (Battaglini et al., 2020a; Berger et al., 2018; Moliadze et al., 2019; Wischnewski et al., 2020) frequency bands, reporting either higher power in the stimulated band after tACS or no effects. Generating hypotheses about the presence and/or direction of tACS aftereffects in RS EEG is not straightforward. In a previous study, with an identical task and very similar experimental design to the present one employing a monolateral right parietal montage in which 18 Hz tACS was applied at 0.8 mA peak-to-baseline intensity, we found an increased beta power after the stimulation (Battaglini et al., 2020a). In the present study the same stimulation was applied in-phase in two locations (P3 and P4), with a peak-to-baseline intensity of 0.8 mA for each site for a total amount of 1.6 mA applied current. Differently, we found a decrease in beta-band power (Fig. 3f).

Only few studies showed that the magnitude of alpha tACS aftereffects can be modulated by tACS intensity, but none of them reported power reduction in the alpha band (De Koninck et al., 2021; Neuling et al., 2015; Wang et al., 2022) and no study at all investigated the possible modulations of RS-EEG induced by beta tACS at different intensities. Considering the possible impact that tACS at different

intensities might have on behavioural performance, it is reasonable to think that it might differentially impact EEG aftereffects too. Another important difference between the present study and (Battaglini et al., 2020a) concerns the bilaterality of tACS montage (vs unilaterality), which resulted in an evident behavioural enhancement in both visual hemifields. However, bilateral high-definition tACS protocols might impact endogenous neural oscillations differently as compared to unilateral protocols, for example by modulating connectivity between the stimulated sites (Helfrich et al., 2014a; Salamanca-Giron et al., 2021; Schwab et al., 2019).

It is important to acknowledge that in the present study a control stimulation frequency was not included. This choice was motivated by the fact that in our previous study (Battaglini et al. 2020b) we showed no effects of right parietal alpha (10 Hz) tACS in modulating threshold in an identical task or post-tACS oscillatory activity, while right parietal beta (18 Hz) tACS did so. Therefore including a condition employing alpha, or other frequencies, as control stimulations would have possibly complicated the experimental design and enlarged the required sample size. In addition, it is not infrequent that tACS, rTMS or otDCS (oscillatory tDCS) applied at a specific frequency results in modulations of oscillatory activity in frequency bands other than the stimulated one (Veniero et al., 2015). In fact, as in the case of nested oscillations (Wischnewski et al., 2023), specific cognitive functions underlying a variety of tasks might depend on the interaction of multiple frequency bands.

4.3. Individual differences in RS-EEG aftereffects

One crucial aspect to determine direction and magnitude of tACS-induced EEG aftereffects is state-dependence, which refers to the relationship of the stimulation parameters and the “state” of the brain during the stimulation, as well as the related individual differences

(Alagapan et al., 2016; Feurra et al., 2019; Lefebvre et al., 2017; Pariz et al., 2023). Previous studies suggested that the “natural frequency” of parietal cortices is the beta band (Capilla et al., 2022; Samaha et al., 2017), but to generate accurate predictions about magnitude and direction of the EEG aftereffects it is necessary to tap into the two main approaches for modelling offline tACS impact: i) neuronal entrainment and ii) spike timing dependent plasticity (STDP).

Neuronal entrainment refers to the imposition of phase resets by an external periodic (sensory or electrical) stimulation on brain oscillations, which results in phase coupling between the two (Fröhlich and McCormick, 2010; Lakatos et al., 2019). Several studies provided evidence for neuronal entrainment via behavioural (Helfrich et al., 2014b; Laczó et al., 2012; Strüber et al., 2014) and electrophysiological measures (Helfrich et al., 2014b). Neuronal entrainment would ultimately lead to enhanced power at the stimulation frequency during its application (i.e., online) (Ali et al., 2013; Pikovsky et al., 2001), which could also last for several minutes afterwards (i.e., offline) (Kasten et al., 2016).

STDP instead, refers to the dependency between the outcome of synaptic changes from the exact timing of their input: when the stimulation frequency is lower than the natural frequency of the addressed network, then pre-synaptic potentials temporally precede post-synaptic potentials, leading to long term potentiation, while the opposite occurs when the stimulation frequency is higher than the natural frequency (Veniero et al., 2015; Vossen et al., 2015; Wischnewski and Schutter, 2017; Zaehle et al., 2010). If such plastic changes are achieved, greater power modulations should be observed at the “natural frequency” and the larger the distance between the natural and the stimulation frequency the larger the power modulations.

Our results showed a linear relationship between the magnitude (i.e. power differences in beta between pre- and post tACS recordings) of the tACS-induced aftereffects in RS-EEG of the BP-tACS condition and the distance from individual beta frequency (IBF): i.e. aftereffects magnitude was larger for beta frequencies lower than IBF while it became smaller for frequencies higher than IBF. Contrarily, no relation was found between aftereffects magnitude and the distance from stimulation frequency (SF) or the difference between IBF and SF (Fig. 4). Furthermore, these results did not show any peak within the beta-band in aftereffects magnitude neither at SF, as predicted by the entrainment account, nor at IBF, as predicted by STDP. The STPD account also predicts a linear relationship between aftereffects magnitude and the distance between IBF and SF, which was not found. Overall, this analysis on individual differences suggest that the stimulation aftereffects reported here can be at least partially attributed to tACS-induced plastic changes across parietal cortices.

4.4. The importance of correcting for aperiodic activity in the study of tACS-induced changes in neural oscillations

We found that aperiodic activity was decreased in the sham condition between 1 and ~16 Hz, which partly overlaps with the reduction of beta band activity (15- ~20 Hz) in the same condition. Thus, the power reduction observed in the “raw” spectrum (before FOOOF-correction) may be partly due to a reduction of aperiodic activity. Similar reduction of power in the “aperiodic spectrum” was found also for the active stimulations, covering the whole power spectrum (Fig. 3e). Importantly, correcting for aperiodic changes allowed us to show clear aftereffects in RS-EEG beta activity in the BP-tACS condition (Fig. 3f).

Alterations of the aperiodic component of the power spectrum have been associated with changes in the ratio between excitatory and inhibitory currents in the brain (Chini et al., 2021; Gao et al., 2017), which might play a role in different cognitive processes (Thuwal et al., 2021; Waschke et al., 2021) and neurodevelopmental disorders (Manyukhina et al., 2022; Robertson et al., 2019; Turri et al., 2023). Our findings are informative for the investigations on tACS-induced aftereffects, showing that taking into account aperiodic changes can reveal

modulation of periodic activity that would remain otherwise undetected or that could be wrongly interpreted.

4.5. Limitations

It is important to acknowledge two considerable limitations of the present study. First, the EEG results we found do not fully support the current theoretical frameworks of tACS-induced after-effects. Infact, the neuronal entrainment theoretical account suggests that power should be higher when recorded at the specific stimulation frequency. Instead, the STDP theoretical account predicts greater power modulations at the “natural frequency” and also that a larger distance between the natural and the stimulation frequency should predict a larger power modulation. We did not observe peaks in beta power nor at the stimulation frequency (18 Hz), as predicted by the entrainment account, nor at the individual beta frequency (IBF), as predicted by the STDP. However, we observed that the magnitude of the aftereffects has a relation with the distance from IBF, being larger at frequencies smaller than IBF, still suggesting the possible presence of plastic changes. Therefore, it is still crucial to precisely understand the neurophysiological effects of tES as well as the impact of different stimulation parameters (e.g., frequency, intensity, duration).

Second, no correlations were found between behavioural results and neurophysiological modulations. This might suggest that the changes observed in physiological activity do not reflect behavioural performance at the individual level. It is possible that as tACS induced after-effects are recorded at rest and not during the crowding task, they might not fully capture the relationship with behavioural outcomes. It is worth mentioning that beta power recorded during (and not before/after) a very similar task to the one employed in the present work, showed a correlation with behavioural performance (Ronconi et al., 2016; Ronconi and Bellacosa Marotti, 2017). Clearly, given that in the present work tACS was applied during the task and given the absence of reliable algorithms to remove tACS artifacts from EEG data, at the present time it is not possible to extract power from EEG data recorded during tACS and explore the presence of possible relationship with behavioural performance. Future studies will hopefully develop methods to overcome this methodological limitation and give important insights for the study of the relation between online tACS-induced physiological modifications and behaviour.

5. Conclusions and clinical implications

The present work provided evidence for the direct relationship between beta oscillations in bilateral parietal cortices and visual crowding during letter identification. The possibility of reducing the impact of visual crowding during letter identification by modulating beta-band activity in parietal cortices via tACS could provide meaningful insights for the development of new neurorehabilitative approaches. Specifically, such novel approaches might particularly benefit individuals with neurological and neurodevelopmental disorders characterised by excessive visual crowding, such as dyslexia (Bertoni et al., 2019; Gori and Facoetti, 2015; Zorzi et al., 2012) and amblyopia (Bonneh et al., 2007).

Data statement

The data of this study are available from the corresponding authors upon reasonable request and data sharing agreement stipulated with the ethical committee which approved the study protocol.

CRediT authorship contribution statement

Giuseppe Di Dona: Writing – review & editing, Writing – original draft, Visualization, Validation, Software, Methodology, Investigation, Formal analysis, Data curation. **Denisa Adina Zamfira:** Writing –

review & editing, Writing – original draft, Validation, Methodology, Investigation, Formal analysis, Data curation. **Martina Battista:** Writing – review & editing, Investigation, Data curation. **Luca Battaglini:** Writing – review & editing, Software, Conceptualization. **Daniela Perani:** Writing – review & editing, Supervision, Resources, Project administration. **Luca Ronconi:** Writing – review & editing, Writing – original draft, Validation, Supervision, Software, Resources, Project administration, Methodology, Funding acquisition, Formal analysis, Data curation, Conceptualization.

Declaration of competing interest

None.

Data availability

The answer has been uploaded as a separate file and indicated in the Data Statement section of the manuscript.

Acknowledgements

This work received financial support from ‘Fondazione Regionale per la Ricerca Biomedica’ of the Region Lombardy (Early Career Award Grant to L.R.; ID: 1751150).

Supplementary materials

Supplementary material associated with this article can be found, in the online version, at [doi:10.1016/j.neuroimage.2024.120550](https://doi.org/10.1016/j.neuroimage.2024.120550).

References

- Aktürk, T., de Graaf, T.A., Güntekin, B., Hanoğlu, L., Sack, A.T., 2022. Enhancing memory capacity by experimentally slowing theta frequency oscillations using combined EEG-tACS. *Sci. Rep.* 12 (1), 14199. <https://doi.org/10.1038/s41598-022-18665-z>.
- Alagapan, S., Schmidt, S.L., Lefebvre, J., Hadar, E., Shin, H.W., Fröhlich, F., 2016. Modulation of cortical oscillations by low-frequency direct cortical stimulation is state-dependent. *PLoS Biol.* 14 (3), e1002424. <https://doi.org/10.1371/journal.pbio.1002424>.
- Albonico, A., Martelli, M., Bricolo, E., Frasson, E., Daini, R., 2018. Focusing and orienting spatial attention differently modulate crowding in central and peripheral vision. *J. Vis.* 18 (3), 4. <https://doi.org/10.1167/18.3.4>.
- Ali, M.M., Sellers, K.K., Fröhlich, F., 2013. Transcranial alternating current stimulation modulates large-scale cortical network activity by network resonance. *J. Neurosci.* 33 (27), 11262–11275. <https://doi.org/10.1523/JNEUROSCI.5867-12.2013>.
- Antal, A., Alekseichuk, I., Bikson, M., Brockmüller, J., Brunoni, A.R., Chen, R., Cohen, L. G., Douthwaite, G., Ellrich, J., Flöel, A., Fregni, F., George, M.S., Hamilton, R., Haeuelsen, J., Herrmann, C.S., Hummel, F.C., Lefaucher, J.P., Liebetanz, D., Luo, C. K., Paulus, W., 2017. Low intensity transcranial electric stimulation: safety, ethical, legal regulatory and application guidelines. *Clin. Neurophysiol.* 128 (9), 1774–1809. <https://doi.org/10.1016/j.clinph.2017.06.001>.
- Atilgan, N., Yu, S.M., He, S., 2020. Visual crowding effect in the parvocellular and magnocellular visual pathways. *J. Vis.* 20 (8), 6. <https://doi.org/10.1167/jov.20.8.6>.
- Bacigalupo, F., Luck, S.J., 2015. The allocation of attention and working memory in visual crowding. *J. Cogn. Neurosci.* 27 (6), 1180–1193. <https://doi.org/10.1162/jocn.a.00771>.
- Bar, M., Kassam, K.S., Ghuman, A.S., Boshyan, J., Schmid, A.M., Dale, A.M., Hämäläinen, M.S., Marinkovic, K., Schacter, D.L., Rosen, B.R., Halgren, E., 2006. Top-down facilitation of visual recognition. *Proc. Natl. Acad. Sci.* 103 (2), 449–454. <https://doi.org/10.1073/pnas.0507062103>.
- Bar, M., Tootell, R.B., Schacter, D.L., Greve, D.N., Fischl, B., Mendola, J.D., Rosen, B.R., Dale, A.M., 2001. Cortical mechanisms specific to explicit visual object recognition. *Neuron* 29 (2), 529–535.
- Battaglini, L., Ghiani, A., Casco, C., Ronconi, L., 2020a. Parietal tACS at beta frequency improves vision in a crowding regime. *Neuroimage* 208, 116451. <https://doi.org/10.1016/j.neuroimage.2019.116451>.
- Battaglini, L., Mena, F., Ghiani, A., Casco, C., Melcher, D., Ronconi, L., 2020b. The effect of alpha tACS on the temporal resolution of visual perception. *Front. Psychol.* 11, 1765. <https://doi.org/10.3389/fpsyg.2020.01765>.
- Battelli, L., Pascual-Leone, A., Cavanagh, P., 2007. The ‘when’ pathway of the right parietal lobe. *Trends Cogn. Sci. (Regul. Ed.)* 11 (5), 204–210. <https://doi.org/10.1016/j.tics.2007.03.001>.
- Bell, A.J., Sejnowski, T.J., 1995. An information-maximization approach to blind separation and blind deconvolution. *Neural Comput.* 7 (6), 1129–1159. <https://doi.org/10.1162/neco.1995.7.6.1129>.
- Berger, A., Pixa, N.H., Steinberg, F., Doppelmayr, M., 2018. Brain oscillatory and hemodynamic activity in a bimanual coordination task following transcranial alternating current stimulation (tACS): a combined EEG-fNIRS study. *Front. Behav. Neurosci.* 12, 67. <https://doi.org/10.3389/fnbeh.2018.00067>.
- Bertoni, S., Franceschini, S., Ronconi, L., Gori, S., Facoetti, A., 2019. Is excessive visual crowding causally linked to developmental dyslexia? *Neuropsychologia* 130, 107–117. <https://doi.org/10.1016/j.neuropsychologia.2019.04.018>.
- Bonneh, Y.S., Sagi, D., Polat, U., 2007. Spatial and temporal crowding in amblyopia. *Vision Res.* 47 (14), 1950–1962. <https://doi.org/10.1016/j.visres.2007.02.015>.
- Boshra, R., Kastner, S., 2022. Attention control in the primate brain. *Curr. Opin. Neurobiol.* 76, 102605. <https://doi.org/10.1016/j.conb.2022.102605>.
- Braddick, O., Atkinson, J., Wattam-Bell, J., 2003. Normal and anomalous development of visual motion processing: motion coherence and ‘dorsal-stream vulnerability’. *Neuropsychologia* 41 (13), 1769–1784. [https://doi.org/10.1016/S0028-3932\(03\)00178-7](https://doi.org/10.1016/S0028-3932(03)00178-7).
- Brainard, D.H., 1997. The psychophysics toolbox. *Spat. Vis.* 10 (4), 433–436.
- Cabral-Calderin, Y., Wilke, M., 2020. Probing the link between perception and oscillations: lessons from transcranial alternating current stimulation. *Neuroscientist* 26 (1), 57–73.
- Capilla, A., Arana, L., García-Huésca, M., Melcón, M., Gross, J., Campo, P., 2022. The natural frequencies of the resting human brain: an MEG-based atlas. *Neuroimage* 258, 119373.
- Capotosto, P., Babiloni, C., Romani, G.L., Corbetta, M., 2009. Frontoparietal cortex controls spatial attention through modulation of anticipatory alpha rhythms. *J. Neurosci.* 29 (18), 5863–5872. <https://doi.org/10.1523/JNEUROSCI.0539-09.2009>.
- Chakravarthi, R., Cavanagh, P., 2009. Bilateral field advantage in visual crowding. *Vision Res.* 49 (13), 1638–1646. <https://doi.org/10.1016/j.visres.2009.03.026>.
- Chakravarthi, R., Pelli, D.G., 2011. The same binding in contour integration and crowding. *J. Vis.* 11 (8) <https://doi.org/10.1167/11.8.10>, 10–10.
- Chen, J., He, Y., Zhu, Z., Zhou, T., Peng, Y., Zhang, X., Fang, F., 2014. Attention-dependent early cortical suppression contributes to crowding. *J. Neurosci.* 34 (32), 10465–10474. <https://doi.org/10.1523/JNEUROSCI.1140-14.2014>.
- Chicherov, V., Plomp, G., Herzog, M.H., 2014. Neural correlates of visual crowding. *Neuroimage* 93, 23–31. <https://doi.org/10.1016/j.neuroimage.2014.02.021>.
- Chini, M., Pfeiffer, T., Hanganu-Opatz, I.L., 2021. Developmental increase of inhibition drives decorrelation of neural activity [Preprint] *Neuroscience*. <https://doi.org/10.1101/2021.07.06.451299>.
- Corbetta, M., Kincade, J.M., Ollinger, J.M., McAvoy, M.P., Shulman, G.L., 2000. Voluntary orienting is dissociated from target detection in human posterior parietal cortex. *Nat. Neurosci.* 3 (3), 292–297. <https://doi.org/10.1038/73009>.
- Corbetta, M., Patel, G., Shulman, G.L., 2008. The reorienting system of the human brain: from environment to theory of mind. *Neuron* 58 (3), 306–324. <https://doi.org/10.1016/j.neuron.2008.04.017>.
- Corbetta, M., Shulman, G.L., 2002. Control of goal-directed and stimulus-driven attention in the brain. *Nature Rev. Neurosci.* 3 (3), 201–215.
- Corbetta, M., Shulman, G.L., 2011. Spatial neglect and attention networks. *Annu. Rev. Neurosci.* 34, 569–599.
- Costa, G.N., Duarte, J.V., Martins, R., Wibrál, M., Castelo-Branco, M., 2017. Interhemispheric binding of ambiguous visual motion is associated with changes in beta oscillatory activity but not with gamma range synchrony. *J. Cogn. Neurosci.* 29 (11), 1829–1844. <https://doi.org/10.1162/jocn.a.01158>.
- De Koninck, B.P., Guay, S., Blais, H., De Beaumont, L., 2021. Parametric study of transcranial alternating current stimulation for brain alpha power modulation. *Brain Commun.* 3 (2), fcab010. <https://doi.org/10.1093/braincomms/fcab010>.
- Delorme, A., Makeig, S., 2004. EEGLAB: an open source toolbox for analysis of single-trial EEG dynamics including independent component analysis. *J. Neurosci. Methods* 134 (1), 9–21. <https://doi.org/10.1016/j.jneumeth.2003.10.009>.
- Di Dona, G., Ronconi, L., 2023. Beta oscillations in vision: a (preconscious) neural mechanism for the dorsal visual stream? *Front. Psychol.* 14, 1296483. <https://doi.org/10.3389/fpsyg.2023.1296483>.
- Donner, T.H., Siegel, M., Oostenveld, R., Fries, P., Bauer, M., Engel, A.K., 2007. Population activity in the human dorsal pathway predicts the accuracy of visual motion detection. *J. Neurophysiol.* 98 (1), 345–359. <https://doi.org/10.1152/jn.01141.2006>.
- Donoghue, T., Haller, M., Peterson, E.J., Varma, P., Sebastian, P., Gao, R., Noto, T., Lara, A.H., Wallis, J.D., Knight, R.T., Shetyuk, A., Voytek, B., 2020. Parameterizing neural power spectra into periodic and aperiodic components. *Nat. Neurosci.* 23 (12), 1655–1665. <https://doi.org/10.1038/s41593-020-00744-x>.
- Ehm, W., Bach, M., Kornmeier, J., 2011. Ambiguous figures and binding: EEG frequency modulations during multistable perception. *Psychophysiology* 48 (4), 547–558.
- Erdfelder, E., Faul, F., Buchner, A., 1996. GPOWER: a general power analysis program. *Behav. Res. Methods Instrum. Comput.* 28, 1–11.
- Fertonani, A., Ferrari, C., Miniussi, C., 2015. What do you feel if I apply transcranial electric stimulation? Safety, sensations and secondary induced effects. *Clin. Neurophysiol.* 126 (11), 2181–2188. <https://doi.org/10.1016/j.clinph.2015.03.015>.
- Feurra, M., Blagovetchenski, E., Nikulin, V.V., Nazarova, M., Lebedeva, A., Pozdeeva, D., Yurevich, M., Rossi, S., 2019. State-dependent effects of transcranial oscillatory currents on the motor system during action observation. *Sci. Rep.* 9 (1), 12858. <https://doi.org/10.1038/s41598-019-49166-1>.
- Fortenbaugh, F.C., Silver, M.A., Robertson, L.C., 2015. Individual differences in visual field shape modulate the effects of attention on the lower visual field advantage in crowding. *J. Vis.* 15 (2) <https://doi.org/10.1167/15.2.19>, 19–19.

- Freeman, J., Simoncelli, E.P., 2011. Metamers of the ventral stream. *Nat. Neurosci.* 14 (9), 1195–1201.
- Fröhlich, F., McCormick, D.A., 2010. Endogenous electric fields may guide neocortical network activity. *Neuron* 67 (1), 129–143. <https://doi.org/10.1016/j.neuron.2010.06.005>.
- Galloto, S., Schuhmann, T., Duecker, F., Middag-van Spanje, M., de Graaf, T.A., Sack, A. T., 2022. Concurrent frontal and parietal network TMS for modulating attention. *iScience* 25 (3), 103962. <https://doi.org/10.1016/j.isci.2022.103962>.
- Gao, R., Peterson, E.J., Voytek, B., 2017. Inferring synaptic excitation/inhibition balance from field potentials. *Neuroimage* 158, 70–78. <https://doi.org/10.1016/j.neuroimage.2017.06.078>.
- Giesbrecht, B., Woldorff, M.G., Song, A.W., Mangun, G.R., 2003. Neural mechanisms of top-down control during spatial and feature attention. *Neuroimage* 19 (3), 496–512. [https://doi.org/10.1016/S1053-8119\(03\)00162-9](https://doi.org/10.1016/S1053-8119(03)00162-9).
- Goldman-Rakic, P.S., Porrino, L.J., 1985. The primate mediodorsal (MD) nucleus and its projection to the frontal lobe. *J. Comp. Neurol.* 242 (4), 535–560.
- Gori, S., Facoetti, A., 2015. How the visual aspects can be crucial in reading acquisition: the intriguing case of crowding and developmental dyslexia. *J. Vis.* 15 (1), 8–8.
- Han, Q., Luo, H., 2019. Visual crowding involves delayed frontoparietal response and enhanced top-down modulation. *Eur. J. Neurosci.* 50 (6), 2931–2941. <https://doi.org/10.1111/ejn.14401>.
- He, S., Cavanagh, P., Intriligator, J., 1996. Attentional resolution and the locus of visual awareness. *Nature* 383 (6598), 334–337.
- Helfrich, R.F., Knepper, H., Nolte, G., Strüber, D., Rach, S., Herrmann, C.S., Schneider, T. R., Engel, A.K., 2014a. Selective modulation of interhemispheric functional connectivity by HD-tACS shapes perception. *PLoS Biol.* 12 (12), e1002031 <https://doi.org/10.1371/journal.pbio.1002031>.
- Helfrich, R.F., Schneider, T.R., Rach, S., Trautmann-Lengsfeld, S.A., Engel, A.K., Herrmann, C.S., 2014b. Entrainment of brain oscillations by transcranial alternating current stimulation. *Curr. Biol.* 24 (3), 333–339. <https://doi.org/10.1016/j.cub.2013.12.041>.
- Heilman, K.M., Van Den Abell, T., 1980. Right hemisphere dominance for attention: the mechanism underlying hemispheric asymmetries of inattention (neglect). *Neurology* 30 (3), 327–330. <https://doi.org/10.1212/wnl.30.3.327>.
- Intriligator, J., Cavanagh, P., 2001. The spatial resolution of visual attention. *Cogn. Psychol.* 43 (3), 171–216.
- Kasten, F.H., Dowsett, J., Herrmann, C.S., 2016. Sustained aftereffect of α -tACS Lasts Up to 70 min after stimulation. *Front. Hum. Neurosci.* 10 <https://doi.org/10.3389/fnhum.2016.00245>.
- Kewan-Khalayly, B., Migó, M., Yashar, A., 2022. Transient attention equally reduces visual crowding in radial and tangential axes. *J. Vis.* 22 (9), 3. <https://doi.org/10.1167/jov.22.9.3>.
- Kleinert, M.-L., Szymanski, C., Müller, V., 2017. Frequency-unspecific effects of θ -tACS related to a visuospatial working memory task. *Front. Hum. Neurosci.* 11, 367. <https://doi.org/10.3389/fnhum.2017.00367>.
- Kornmeier, J., Bach, M., 2012. Ambiguous figures—what happens in the brain when perception changes but not the stimulus. *Front. Hum. Neurosci.* 6, 51.
- Laczó, B., Antal, A., Niebergall, R., Treue, S., Paulus, W., 2012. Transcranial alternating stimulation in a high gamma frequency range applied over V1 improves contrast perception but does not modulate spatial attention. *Brain Stimul.* 5 (4), 484–491.
- Lakatos, P., Gross, J., Thut, G., 2019. A new unifying account of the roles of neuronal entrainment. *Curr. Biol.* 29 (18), R890–R905. <https://doi.org/10.1016/j.cub.2019.07.075>.
- Lamme, V.A.F., Roelfsema, P.R., 2000. The distinct modes of vision offered by feedforward and recurrent processing. *Trends Neurosci.* 23 (11), 571–579. [https://doi.org/10.1016/S0166-2236\(00\)01657-X](https://doi.org/10.1016/S0166-2236(00)01657-X).
- Lefebvre, J., Hutt, A., Fröhlich, F., 2017. Stochastic resonance mediates the state-dependent effect of periodic stimulation on cortical alpha oscillations. *Elife* 6, e32054. <https://doi.org/10.7554/eLife.32054>.
- Lenth, R., Singmann, H., Love, J., Buerkner, P., Herve, M., 2018. Emmeans: estimated marginal means, aka least-squares means. *R Package Version 1* (1), 3.
- Levi, D.M., 2008. Crowding—an essential bottleneck for object recognition: a mini-review. *Vision Res.* 48 (5), 635–654.
- Levi, D.M., Hariharan, S., Klein, S.A., 2002. Suppressive and facilitatory spatial interactions in peripheral vision: peripheral crowding is neither size invariant nor simple contrast masking. *J. Vis.* 2 (2) <https://doi.org/10.1167/2.2.3>, 3–3.
- Levy, T., Walsh, V., Lavidor, M., 2010. Dorsal stream modulation of visual word recognition in skilled readers. *Vision Res.* 50 (9), 883–888. <https://doi.org/10.1016/j.visres.2010.02.019>.
- Linares, D., López i Moliner, J., 2016. quickpsy: an R package to fit psychometric functions for multiple groups. *R. J.* 8 (1), 122–131. 2016 num.
- Manyukhina, V.O., Prokofyev, A.O., Galuta, I.A., Goiaeva, D.E., Obukhova, T.S., Schneiderman, J.F., Altkhov, D.I., Stroganova, T.A., Orekhova, E.V., 2022. Globally elevated excitation–inhibition ratio in children with autism spectrum disorder and below-average intelligence. *Mol. Autism.* 13 (1), 20. <https://doi.org/10.1186/s13229-022-00498-2>.
- Maris, E., Oostenveld, R., 2007. Nonparametric statistical testing of EEG- and MEG-data. *J. Neurosci. Methods* 164 (1), 177–190.
- Maunsell, J.H., Newsome, W.T., 1987. Visual processing in monkey extrastriate cortex. *Annu. Rev. Neurosci.* 10 (1), 363–401.
- Mengotti, P., Käsbauer, A.S., Fink, G.R., Vossel, S., 2020. Lateralization, functional specialization, and dysfunction of attentional networks. *Cortex* 132, 206–222. <https://doi.org/10.1016/j.cortex.2020.08.022>.
- Miller, E.K., Cohen, J.D., 2001. An integrative theory of prefrontal cortex function. *Annu. Rev. Neurosci.* 24 (1), 167–202.
- Moliadze, V., Sierau, L., Lyzhko, E., Stenner, T., Werchowski, M., Siniatchkin, M., Hartwigsen, G., 2019. After-effects of 10Hz tACS over the prefrontal cortex on phonological word decisions. *Brain Stimul.* 12 (6), 1464–1474. <https://doi.org/10.1016/j.brs.2019.06.021>.
- Morrone, M.C., Tosetti, M., Montanaro, D., Fiorentini, A., Cioni, G., Burr, D.C., 2000. A cortical area that responds specifically to optic flow, revealed by fMRI. *Nat. Neurosci.* 3 (12), 1322–1328. <https://doi.org/10.1038/81860>.
- Neuling, T., Ruhnau, P., Fuscà, M., Demarchi, G., Herrmann, C.S., Weisz, N., 2015. Friends, not foes: magnetoencephalography as a tool to uncover brain dynamics during transcranial alternating current stimulation. *Neuroimage* 118, 406–413. <https://doi.org/10.1016/j.neuroimage.2015.06.026>.
- Okazaki, M., Kaneko, Y., Yumoto, M., Arima, K., 2008. Perceptual change in response to a bistable picture increases neuromagnetic beta-band activities. *Neurosci. Res.* 61 (3), 319–328.
- Oostenveld, R., Fries, P., Maris, E., Schoffelen, J.-M., 2011. FieldTrip: open source software for advanced analysis of MEG, EEG, and invasive electrophysiological data. *Comput. Intell. Neurosci.* 2011, 1–9. <https://doi.org/10.1155/2011/156869>.
- Pahor, A., Jaušovec, N., 2018. The effects of theta and gamma tACS on working memory and electrophysiology. *Front. Hum. Neurosci.* 11, 651. <https://doi.org/10.3389/fnhum.2017.00651>.
- Pariz, A., Trotter, D., Hutt, A., Lefebvre, J., 2023. Selective control of synaptic plasticity in heterogeneous networks through transcranial alternating current stimulation (tACS). *PLoS Comput. Biol.* 19 (4), e1010736 <https://doi.org/10.1371/journal.pcbi.1010736>.
- Parkes, L., Lund, J., Angelucci, A., Solomon, J.A., Morgan, M., 2001. Compulsory averaging of crowded orientation signals in human vision. *Nat. Neurosci.* 4 (7), 739–744.
- Pelli, D.G., 2008. Crowding: a cortical constraint on object recognition. *Curr. Opin. Neurobiol.* 18 (4), 445–451.
- Pelli, D.G., Palomares, M., Majaj, N.J., 2004. Crowding is unlike ordinary masking: distinguishing feature integration from detection. *J. Vis.* 4 (12), 12–12.
- Peng, C., Hu, C., Chen, Y., 2018. The temporal dynamic relationship between attention and crowding: electrophysiological evidence from an event-related potential study. *Front. Neurosci.* 12, 844. <https://doi.org/10.3389/fnins.2018.00844>.
- Pikovsky, A., Rosenblum, M., Kurths, J., 2001. A universal concept in nonlinear sciences. *Self.* 2, 3.
- Pion-Tonachini, L., Kreutz-Delgado, K., Makeig, S., 2019. ICLabel: an automated electroencephalographic independent component classifier, dataset, and website. *Neuroimage* 198, 181–197. <https://doi.org/10.1016/j.neuroimage.2019.05.026>.
- Rempel-Clower, N.L., Barbass, H., 2000. The laminar pattern of connections between prefrontal and anterior temporal cortices in the rhesus monkey is related to cortical structure and function. *Cerebral Cortex* 10 (9), 851–865.
- Ringer, R.V., Coy, A.M., Larson, A.M., Loschky, L.C., 2021. Investigating visual crowding of objects in complex real-world scenes. *Perception* 12 (2), 204166952199415. <https://doi.org/10.1177/2041669521994150>.
- Robertson, M.M., Furlong, S., Voytek, B., Donoghue, T., Boettiger, C.A., Sheridan, M.A., 2019. EEG power spectral slope differs by ADHD status and stimulant medication exposure in early childhood. *J. Neurophysiol.* 122 (6), 2427–2437. <https://doi.org/10.1152/jn.00388.2019>.
- Rogala, J., Kublik, E., Krauz, R., Wróbel, A., 2020. Resting-state EEG activity predicts frontoparietal network reconfiguration and improved attentional performance. *Sci. Rep.* 10 (1), 5064. <https://doi.org/10.1038/s41598-020-61866-7>.
- Romei, V., Driver, J., Schyns, P.G., Thut, G., 2011. Rhythmic TMS over parietal cortex links distinct brain frequencies to global versus local visual processing. *Curr. Biol.* 21 (4), 334–337. <https://doi.org/10.1016/j.cub.2011.01.035>.
- Ronconi, L., Bellacosa Marotti, R., 2017. Awareness in the crowd: beta power and alpha phase of prestimulus oscillations predict object discrimination in visual crowding. *Conscious. Cogn.* 54, 36–46. <https://doi.org/10.1016/j.concog.2017.04.020>.
- Ronconi, L., Bertoni, S., Bellacosa Marotti, R., 2016. The neural origins of visual crowding as revealed by event-related potentials and oscillatory dynamics. *Cortex* 79, 87–98. <https://doi.org/10.1016/j.cortex.2016.03.005>.
- Salamanca-Giron, R.F., Raffin, E., Zandvliet, S.B., Seeber, M., Michel, C.M., Sauseng, P., Huxlin, K.R., Hummel, F.C., 2021. Enhancing visual motion discrimination by desynchronizing bifocal oscillatory activity. *Neuroimage* 240, 118299. <https://doi.org/10.1016/j.neuroimage.2021.118299>.
- Samaha, J., Gossesries, O., Postle, B.R., 2017. Distinct oscillatory frequencies underlie excitability of human occipital and parietal cortex. *J. Neurosci.* 37 (11), 2824–2833. <https://doi.org/10.1523/JNEUROSCI.3413-16.2017>.
- Schwab, B.C., Misselhorn, J., Engel, A.K., 2019. Modulation of large-scale cortical coupling by transcranial alternating current stimulation. *Brain Stimul.* 12 (5), 1187–1196. <https://doi.org/10.1016/j.brs.2019.04.013>.
- Stengel, C., Vernet, M., Amengual, J.L., Valero-Cabré, A., 2021. Causal modulation of right hemisphere fronto-parietal phase synchrony with Transcranial Magnetic Stimulation during a conscious visual detection task. *Sci. Rep.* 11 (1), 3807. <https://doi.org/10.1038/s41598-020-79812-y>.
- Strüber, D., Rach, S., Trautmann-Lengsfeld, S.A., Engel, A.K., Herrmann, C.S., 2014. Antiphase 40Hz oscillatory current stimulation affects bistable motion perception. *Brain Topogr.* 27 (1), 158–171. <https://doi.org/10.1007/s10548-013-0294-x>.
- Sun, H.-M., Balas, B., 2015. Face features and face configurations both contribute to visual crowding. *Attention Percep. Psychophys.* 77 (2), 508–519.
- Szczepanski, S.M., Konen, C.S., Kastner, S., 2010. Mechanisms of spatial attention control in frontal and parietal cortex. *J. Neurosci.* 30 (1), 148–160. <https://doi.org/10.1523/JNEUROSCI.3862-09.2010>.
- Thuwal, K., Banerjee, A., Roy, D., 2021. Aperiodic and periodic components of ongoing oscillatory brain dynamics link distinct functional aspects of cognition across adult

- lifespan. *eNeuro* 8 (5). <https://doi.org/10.1523/ENEURO.0224-21.2021>. ENEURO.0224-21.2021.
- Turri, C., Di Dona, G., Santoni, A., Zamfira, D.A., Franchin, L., Melcher, D., Ronconi, L., 2023. Periodic and aperiodic EEG features as potential markers of developmental dyslexia. *Biomedicines* 11 (6), 1607. <https://doi.org/10.3390/biomedicines11061607>.
- Veniero, D., Gross, J., Morand, S., Duecker, F., Sack, A.T., Thut, G., 2021. Top-down control of visual cortex by the frontal eye fields through oscillatory realignment. *Nat. Commun.* 12 (1), 1757. <https://doi.org/10.1038/s41467-021-21979-7>.
- Veniero, D., Vossen, A., Gross, J., Thut, G., 2015. Lasting EEG/MEG aftereffects of rhythmic transcranial brain stimulation: level of control over oscillatory network activity. *Front. Cell Neurosci.* 9 <https://doi.org/10.3389/fncel.2015.00477>.
- Vidyaasagar, T.R., Pammer, K., 2010. Dyslexia: a deficit in visuo-spatial attention, not in phonological processing. *Trends Cogn. Sci. (Regul. Ed.)* 14 (2), 57–63.
- Vossen, A., Gross, J., Thut, G., 2015. Alpha power increase after transcranial alternating current stimulation at alpha frequency (α -tACS) reflects plastic changes rather than entrainment. *Brain Stimul.* 8 (3), 499–508. <https://doi.org/10.1016/j.brs.2014.12.004>.
- Wang, Y., Hou, P., Li, W., Zhang, M., Zheng, H., Chen, X., 2022. The influence of different current-intensity transcranial alternating current stimulation on the eyes-open and eyes-closed resting-state electroencephalography. *Front. Hum. Neurosci.* 16, 934382 <https://doi.org/10.3389/fnhum.2022.934382>.
- Waschke, L., Donoghue, T., Fiedler, L., Smith, S., Garrett, D.D., Voytek, B., Obleser, J., 2021. Modality-specific tracking of attention and sensory statistics in the human electrophysiological spectral exponent. *Elife* 10, e70068. <https://doi.org/10.7554/eLife.70068>.
- Whitney, D., Levi, D.M., 2011. Visual crowding: a fundamental limit on conscious perception and object recognition. *Trends Cogn. Sci. (Regul. Ed.)* 15 (4), 160–168.
- Wischniewski, M., Alekseichuk, I., Opitz, A., 2023. Neurocognitive, physiological, and biophysical effects of transcranial alternating current stimulation. *Trends Cogn. Sci. (Regul. Ed.)* 27 (2), 189–205. <https://doi.org/10.1016/j.tics.2022.11.013>.
- Wischniewski, M., Joergensen, M.L., Compen, B., Schutter, D.J.L.G., 2020. Frontal beta transcranial alternating current stimulation improves reversal learning. *Cerebral Cortex* 30 (5), 3286–3295. <https://doi.org/10.1093/cercor/bhz309>.
- Wischniewski, M., Schutter, D.J., 2017. After-effects of transcranial alternating current stimulation on evoked delta and theta power. *Clin. Neurophysiol.* 128 (11), 2227–2232.
- Yaple, Z., Vakhrushev, R., 2018. Modulation of the frontal-parietal network by low intensity anti-phase 20Hz transcranial electrical stimulation boosts performance in the attentional blink task. *Int. J. Psychophysiol.* 127, 11–16. <https://doi.org/10.1016/j.ijpsycho.2018.02.014>.
- Yordanova, J., Kolev, V., Verleger, R., Heide, W., Grumbt, M., Schürmann, M., 2017. Synchronization of fronto-parietal beta and theta networks as a signature of visual awareness in neglect. *Neuroimage* 146, 341–354. <https://doi.org/10.1016/j.neuroimage.2016.11.013>.
- Zaehle, T., Rach, S., Herrmann, C.S., 2010. Transcranial alternating current stimulation enhances individual alpha activity in human EEG. *PLoS One* 5 (11), e13766. <https://doi.org/10.1371/journal.pone.0013766>.
- Zaretskaya, N., Bartels, A., 2015. Gestalt perception is associated with reduced parietal beta oscillations. *Neuroimage* 112, 61–69. <https://doi.org/10.1016/j.neuroimage.2015.02.049>.
- Zorzi, M., Barbiero, C., Facoetti, A., Lonciari, I., Carrozzi, M., Montico, M., Bravar, L., George, F., Pech-Georgel, C., Ziegler, J.C., 2012. Extra-large letter spacing improves reading in dyslexia. *Proc. Natl. Acad. Sci.* 109 (28), 11455–11459. <https://doi.org/10.1073/pnas.1205566109>.